Available online at www.sciencedirect.com

ScienceDirect

Energy Procedia 75 (2015) 1059 – 1064

Energy Procedia

An Efficient Power Plant Model of Electric Vehicles for Unit Commitment of Large Scale Wind Farms

Mingshen Wang[1], Yunfei Mu[1,*], Hongjie Jia[1], Pingliang Zeng[2], Jianzhong Wu[3], Wanxing Sheng[2]

1. Key Laboratory of Smart Grid of Ministry of Education, Tianjin University, Tianjin 300072, China
2. China Electric Power Research Institute, Beijing 100192, China
3. Institute of Energy, Cardiff University, Cardiff, CF24 3AA, UK

Abstract

An efficient power plant model of electric vehicles (E-EPP) considering the travelling comfort levels of EV users is developed to investigate the contribution of EVs on the unit commitment (UC) of large scale wind farms. Firstly, a generic EV battery model (GEBM) is established considering the uncertainties of battery parameters. Then, a Monte Carlo Simulation (MCS) method is implemented within the E-EPP to obtain the available response capacity of EV charging load over time. And a UC strategy using the E-EPP based on power flow tracing is developed. Finally, a modified IEEE 118-bus system integrated with wind farms is used to verify the effectiveness of the E-EPP for the UC of large scale wind farms.

Keywords: Electric vehicle (EV); Vehicle-to-grid (V2G); Efficient power plant (EPP); Unit commitment (UC); Wind farm

1. Introduction

A number of countries have taken specific initiatives to de-carbonize their electrical power system by encouraging wind generation. In UK, there may be up to 30 GW of wind generation within a total generation capacity of some 100 GW serving a load of around 60 GW by 2020 [1]. A high penetration of wind energy will increase the difficulty in the unit commitment (UC) of power system. Without effective management, the economy of wind power integration will decrease and the system operation cost will increase. As a new kind of controllable load, Electric vehicles (EVs) have the potential to increase the capability of residential consumers to participate in the demand response scheme. Under the vehicle-to-grid (V2G) concept, the EVs can not only act as a rapid responsive load, but also serve as an energy storage system for supporting the operation of power system [2].

In this paper, an efficient power plant model of EVs (E-EPP) is developed to evaluate the real-time available V2G capacity during a day. Under a new developed UC strategy, the E-EPP can respond to the fluctuations of power system caused by the integration of large scale wind farms, which can significantly decrease the frequent power variations of traditional generators. The E-EPP can promote the utilization of wind power and improve the stability of power system.

2. Framework of the efficient power plant model of EVs

The framework of the E-EPP is shown in Fig. 1. Through V2G service, the E-EPP is developed as an integrated aggregator managing a large number of geographically dispersed EVs connected to power system. Based on the market survey data of various EV batteries, a nonlinear generic EV battery model (GEBM) shown in Fig. 2 is established to accurately describe EV charging characteristics. The MERGE EV database provides the characteristics of EV battery type, capacity and energy consumption per kilometer of various EVs intended for the European market [3]. Meanwhile, daily travelling distance and minimum desired State of Charging (SOC) for travelling are obtained based on the sufficient survey data

* Yunfei Mu. Tel.: +86-1582-250-9583; fax: +86-022-27892809.
E-mail address: yunfeimu@tju.edu.cn.

Peer-review under responsibility of Applied Energy Innovation Institute
doi:10.1016/j.egypro.2015.07.471

of vehicle users. From battery capacity, energy consumption per kilometer and daily travelling distance, the initial SOC before charging can be calculated. The uncertain parameters of EV battery type, initial SOC, time of charging and minimum desired SOC for travel are used by the Monte Carlo Simulation (MCS) method for modelling of the E-EPP with its available response capacity.

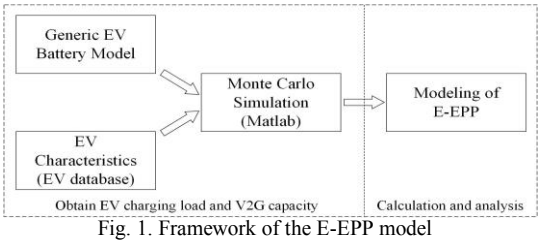

Fig. 1. Framework of the E-EPP model

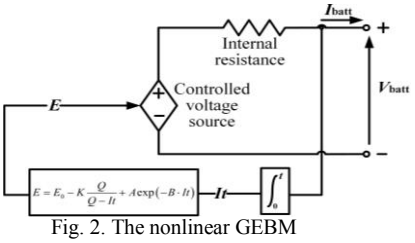

Fig. 2. The nonlinear GEBM

3. Formulation of the E-EPP

3.1. EV Characteristics

A. EV classification

In the formulation of the E-EPP model, EVs are classified into the following two groups.

Based on the type of usage, EVs are classified into three groups, i.e. Home-Based-Work (HBW), Home-Based-Other (HBO) and Non-Home-Based (NHB). Their proportions in UK are 61%, 30% and 9%, respectively [4]. This classification is used to obtain the EV daily travelling distance and time.

According to vehicle type, EVs are classified into four groups, i.e. L7e, M1, N1 and N2. And their proportions are 1.49%, 87.51%, 10% and 1%, respectively [3]. This classification is used to obtain the battery type, capacity and energy consumption per kilometer of a single EV.

B. Battery type, capacity and energy consumption

Based on the market survey data of battery types (B_t) in the UK, four promising batteries applied in EVs are lithium-ion, lead-acid, nickel-metal-hybrid and nickel-cadmium batteries, and their proportions are 50%, 20%, 20% and 10%, respectively [3]. According to the classification of EV using type (L7e, M1, N1 and N2), the distributions of EV battery capacity (Q_e) are shown in Table 1 [3]. Meanwhile, the EV database provides the distributions of energy consumption per kilometer (C_e) as described in Table 2 [3].

Table 1. Distributions of EV battery capacity (kWh)

EV group	L7e	M1	N1	N2
Distribution	Gamma	Gamma	Normal	Normal
Parameter	α=10.8 β=0.8	α=4.5 β=6.7	μ=23.0 σ=9.5	μ=85.3 σ=28.0
Min	3.0	10.0	9.6	51.0
Max	15.0	72.0	40.0	120.0

Table 2. Distributions of energy consumption per kilometre (kWh/km)

C_e	L7e	M1	N1	N2
0.05~0.10	0.34	0.05	0.00	0.00
0.10~0.15	0.58	0.35	0.29	0.00
0.15~0.20	0.08	0.45	0.14	0.00
0.20~0.25	0.00	0.15	0.57	0.00
0.45~0.50	0.00	0.00	0.00	0.50
0.50~0.55	0.00	0.00	0.00	0.25
0.80~0.85	0.00	0.00	0.00	0.25

C. Daily travelling distance and time

Based on the usage type (HBW, HBO and NHB), the probability density function of daily travelling distance (d) is described by (1) [4].

$$f\left(d;\mu_{\mathrm{d}},\sigma_{\mathrm{d}}\right)=\frac{1}{\sqrt{2\pi}\sigma_{\mathrm{d}}}\exp\left(-\frac{\left(d-\mu_{\mathrm{d}}\right)^{2}}{2\sigma_{\mathrm{d}}^{2}}\right) \tag{1}$$

For the HBW and HBO vehicles, the mean travelling distance μ_d is 35.9 km and the standard deviation σ_d is 19.6 km; while for the NHB vehicles, the mean is 87.1 km and the standard deviation is 24.5 km.

Travelling time of EVs mainly depends on the users' travelling habits. The distributions of travelling time shown in Fig. 3 is used to determine the starting time (t_s) and finishing time (t_f) of a single EV [5].

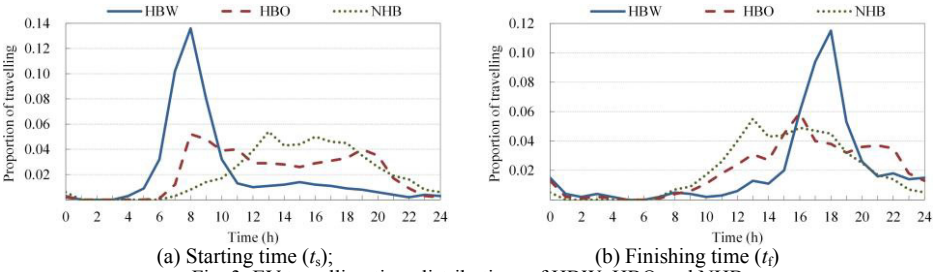

(a) Starting time (t_s); (b) Finishing time (t_f)

Fig. 3. EV travelling time distributions of HBW, HBO and NHB

D. Minimum desired SOC for travelling

SOC_e is defined as the minimum desired SOC for an EV user to finish his daily travel. Based on a sufficient market survey of vehicle users [3], SOC_e described by (2) is modelled stochastically with μ_e equal to 0.6 and σ_e equal to 0.1 within [0.45, 0.8].

$$f\left(SOC_e;\mu_e,\sigma_e\right)=\frac{1}{\sqrt{2\pi}\sigma_e}\exp\left(-\frac{\left(SOC_e-\mu_e\right)^2}{2\sigma_e^2}\right) \tag{2}$$

3.2. A Generic EV Battery Model

In this section, the GEBM, shown in Fig. 2, is developed to describe the charging/discharging characteristics of EV batteries [6]. In this model, SOC is the only state variable for accurately reproducing the manufacturers' discharging curves of four most promising batteries (depicted in section 3.1) in the future EV market.

Assuming a constant charging current I to simplify the integral part in the GEBM, the charging power P is described by (3) and (4).

$$P=V_{batt}I=E_0I-KI/SOC+AI\exp\left(-BIt\right)-RI^2 \tag{3}$$

$$SOC=1-\int Idt/Q \tag{4}$$

where E_0 is battery constant voltage (V); K is polarisation voltage (V); Q is battery capacity (Ah); R is internal resistance (Ω); I is battery current (A); A is exponential zone amplitude (V); B is exponential zone time constant inverse (Ah^{-1}).

3.3. The Formulation of the E-EPP

The E-EPP model is formulated by the following six steps.

Step1: Determine B_t, C_e and Q_e of an individual EV battery

A MCS process is used to generate B_t depending on the proportion of the four promising EV batteries, Q_e based on the distributions and constrains in Table 1, and C_e based on the distributions in Table 2.

Step2: Determine the parameters in the GEBM

It is assumed that the EV battery charging process is reversible. Once B_t and Q_e are determined in step1, the other parameters in the GEBM are deduced from the discharging curves supplied by battery manufacturers [6]. Then the charging process consisting of the charging power (P) and various SOC (SOC) is obtained via the GEBM.

Step3: Determine daily travelling distance and charging starting time

Daily travelling distance (d) is determined by (1) with the MCS process. While charging starting time (t_{sc}) is determined by people's daily transport behaviours. All EVs are assumed to start charging as soon as their daily trips are finished. Thus t_{sc} is equal to t_f that is determined by the distributions in Fig. 3(b).

Step4: Determine the initial SOC (SOC_0) when an EV starts to charge

Assuming the SOC drops linearly with the travelling distance [4], the initial SOC_0 is determined by daily travelling distance (d) and maximum travelling distance (d_t) as shown in (5).

$$SOC_0=\left(\delta-d/d_t\right)\times100\% \tag{5}$$

where δ is the SOC of an EV before driving and it varies within the range of [0.8, 0.9], which helps prolong the lifetime of a battery [3]; the maximum travelling distance is obtained by $d_t=Q_e/C_e$.

Step5: Determine the response state of an EV

Based on the distribution in (2), SOC_e of an EV user is generated with the MCS process. For an individual EV_i, the response state at time t ($\eta_{i,t}$) is determined by (6). If $\eta_{i,t}$ is 0, the charging EV_i is uncontrollable. If $\eta_{i,t}$ is 1, the EV_i can be selected to charge, stop charging or discharge the stored energy back to grid. While if $\eta_{i,t}$ is 2, the EV_i can be chosen to recharge and discharge.

$$\eta_{i,t}=\begin{cases}0, & 0<SOC_{i,t}\le SOC_{i,e}\\ 1, & SOC_{i,e}<SOC_{i,t}\le \delta_i\\ 2, & \delta_i<SOC_{i,t}<100\%\end{cases} \tag{6}$$

Step6: Obtain the E-EPP model

Steps 1~5 are repeated n times for n EVs with the MCS process. The real-time charging power ($P_{\text{E-EPP},t}$) with the upper boundary ($P_{\text{upper},t}$) and lower boundary ($P_{\text{lower},t}$) are determined by (7).

$$\begin{cases}P_{\text{E-EPP},t}=\sum_{i=1}^{l_t}P_{i,t}+\sum_{j=1}^{s_t}P_{j,t}\\ P_{\text{upper},t}=\sum_{i=1}^{l_t}P_{i,t}+\sum_{j=1}^{m_t}P_{j,t}+\sum_{k=1}^{n_t}P_{k,t}\\ P_{\text{lower},t}=\sum_{i=1}^{l_t}P_{i,t}-\sum_{j=1}^{m_t}P_{j,t}-\sum_{k=1}^{n_t}P_{k,t}\end{cases} \tag{7}$$

where $P_{i,t}$ is the charging/discharging power of EV_i at time t; l_t is the number of EVs whose $\eta_{i,t}$ is 0; m_t is the number of EVs whose $\eta_{i,t}$ is 1, and s_t is the number of charging EVs among the m_t EVs; n_t is the number of EVs whose $\eta_{i,t}$ is 2.

4. Implement E-EPP for the unit commitment of wind farms

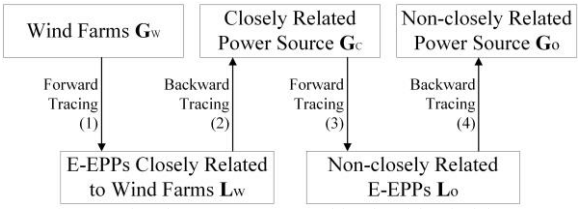

Fig. 4. Related power sources and loads with wind farms

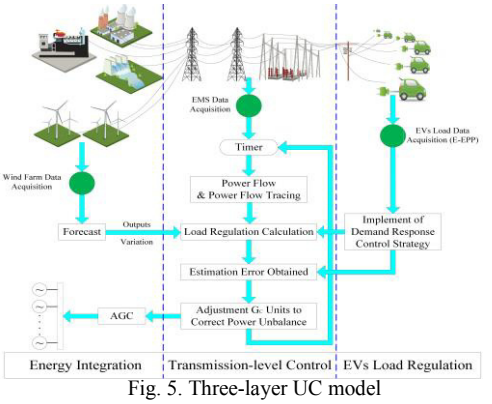

Fig. 5. Three-layer UC model

In order to select the suitable E-EPP for the UC of wind farms, power flow tracing, as shown in Fig. 4, is used to obtain buses closely related with the wind power. Forward power flow tracing can associate power sources with their supplying loads and the corresponding distributing factors, while backward power flow tracing can associate loads with their power sources and corresponding power extracting factors. The E-EPPs in $\mathbf{L}_W$ firstly respond to the intermittent output of wind power, and the variations are then balanced by $\mathbf{G}_C$. Because $\mathbf{G}_C$ supplies the same load in $\mathbf{L}_W$ with $\mathbf{G}_W$. If the remaining unbalance exists, it will be compensated by the E-EPPs in $\mathbf{L}_O$ and the $\mathbf{G}_O$. Fig. 5 shows a three-layer UC model (energy integration layer, transmission-level control layer and load-side regulation layer) with wind farms. Taking power flow tracing of G_{Wp} as an example, specific steps of the UC strategy are listed as follows:

(a) The power flow tracing is utilized to identify the loads in $\mathbf{L}_W$ and generators in $\mathbf{G}_C$. Distributing factor $\gamma_{p,q}$ from G_{Wp} to L_{Wq} and extracting factor $\varphi_{q,r}$ from L_{Wq} to G_{Cr} are calculated by (8).

$$\begin{cases}\gamma_{p,q}=P_{G_{Wp}-L_{Wq}}/P_{G_{Wp}-\mathbf{L}_W}\\ \varphi_{q,r}=P_{L_{Wq}-G_{Cr}}/P_{L_{Wq}-\mathbf{G}_C}\end{cases} \tag{8}$$

where G_{Wp} is the wind farm connecting to bus p in $\mathbf{G}_W$; L_{Wq} is the specific load connecting to bus q in $\mathbf{L}_W$; G_{Cr} is the specific generator connecting to bus r in $\mathbf{G}_C$; $P_{G_{Wp}-L_{Wq}}$ is the power from G_{Wp} to L_{Wq}; $P_{G_{Wp}-\mathbf{L}_W}$ is the power from G_{Wp} to all the loads in $\mathbf{L}_W$; $P_{L_{Wq}-G_{Cr}}$ is the power that L_{Wq} draws from G_{Cr}; $P_{L_{Wq}-\mathbf{G}_C}$ is the total power that L_{Wq} draws from $\mathbf{G}_C$.

(b) Wind power variation ΔP_{Wp} at time t is predicted based on the historical data of wind output. The target power adjust value in L_{Wq} is calculated by $\gamma_{p,q}\Delta P_{Wp}$.

(c) The actual power P_{Eq} (constrained by the boundary of E-EPP$_q$ belonging to L_{Wq}) undertaken by the E-EPP$_q$ in L_{Wq} is determined. Compared with the value of $\gamma_{p,q}\Delta P_{Wp}$ in step (b), the unbalanced power ΔP_{Cq} ($\gamma_{p,q}\Delta P_{Wp}$-$P_{Eq}$) is compensated by $\mathbf{G}_C$, and the compensation value of G_{Cr} is given by $\varphi_{q,r}\Delta P_{Cq}$.

5. Case studies and simulation results

Fig. 6 gives the sub-area I of an IEEE 118-bus system, which connects with sub-area II and sub-area III through tie-lines of 15-33, 19-34 and 23-24, 30-38. A wind farm with an installed capacity of 300 MW is integrated at bus 117. According to the results of power flow tracing, the closely related $\mathbf{L}_W$ and $\mathbf{G}_C$ are L12, L13, L14, L15, L16 and G10, G12. The E-EPPs in $\mathbf{L}_W$ will replace part of the generators in $\mathbf{G}_C$ to respond to wind power fluctuations, and the number of EVs in corresponding $\mathbf{L}_W$ is shown in Table 3.

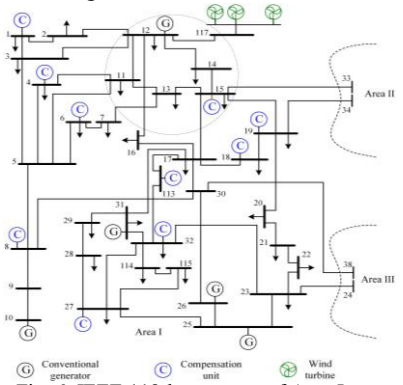

Fig. 6. IEEE 118-bus system of Area I

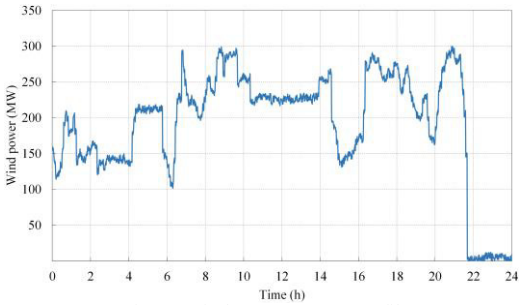

Fig. 7. Wind power output profile

Table 3. Number of EVs for simulation

Number of EVs at closely related buses				
L12	L13	L14	L15	L16
1880	1360	560	3600	1000

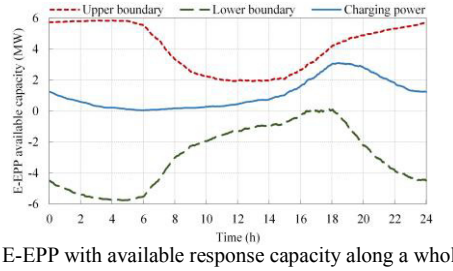

Fig. 8. E-EPP with available response capacity along a whole day

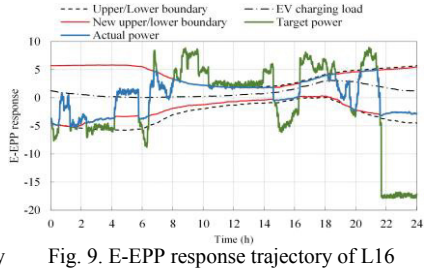

Fig. 9. E-EPP response trajectory of L16

A typical wind output profile of one-min recorded in UK is shown in Fig. 7. Fig. 8 gives the E-EPP of aggregate EVs at L16. According to the E-EPP model and the UC strategy, the simulation results are shown in Fig. 9. The output of G10 and G12 following the wind power's fluctuation is shown in Fig. 10. And the following conclusions are given:

(1) From Fig. 9, it is clear that the E-EPP of L16 responds to the variations of wind power. Under the UC strategy, when the target power is within the new boundary, the actual EV charging power can follow the target power accurately. When the target power is beyond the boundary, the actual response capacity of E-EPP is limited.

(2) As the E-EPP participates in the UC, the traditional generators only provide the remaining

unbalanced power which is beyond the available capacity of E-EPP. Both the frequency and the capacity of traditional generators used for UC are decreased. In this case, the output of G10 varies from 382.7 MW to 618.2 MW and the maximum power change is 148.8 MW without the support from E-EPP. With the E-EPP participating in the UC strategy, the output of G10 is within [402.2 MW, 594.0 MW] and the maximum power change decreases to 130.9 MW. G12 has the similar effect with G10. For comparison purpose, the probability distributions (for power output variations) of G10 and G12 are shown in Fig. 11. It is clear that the power variations of G10 and G12 are decreased with the proposed UC strategy.

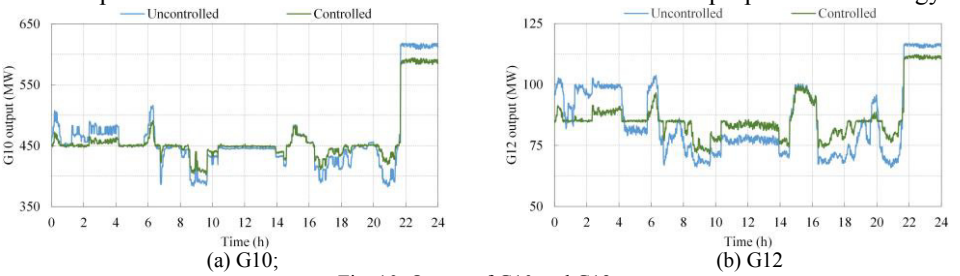

(a) G10; (b) G12

Fig. 10. Output of G10 and G12

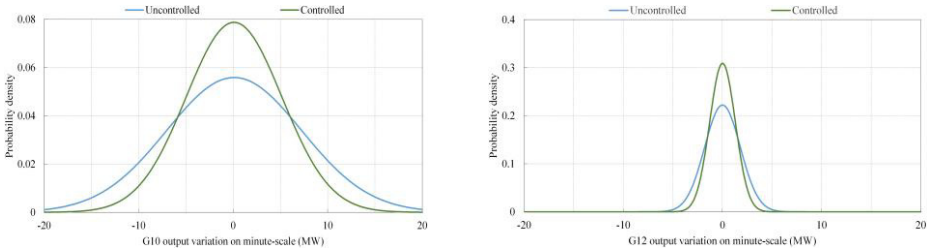

(a) G10; (b) G12

Fig. 11. Probability distributions of G10 and G12 output variations

6. Conclusions

An E-EPP model is developed to evaluate the V2G capacity along a typical day considering EV users' travelling comfort levels. A MCS method is developed within the E-EPP to obtain the EV charging load with its available capacity along a day. And a UC strategy using the E-EPP based on power flow tracing is developed. A modified IEEE 118-bus system integrated with large scale wind farms is used to verify the available V2G response capacity of E-EPP during a day. The E-EPP is used for the UC of wind farms which can decrease the power output variations of traditional generators, which can significantly promote the wide application of wind farms and support the development of low carbon economy.

Acknowledgements

This work is supported in part by China-UK NSFC/EPSRC EV (Grant No. 51361130152 and EP/L001039/1), the project National Natural Science Foundation of China (Grant No. 51307115, 51377117, and 51277128), the National High Technology R&D Program (863) of China (Grant No. 2014AA051901), Special funding for "Thousands Plan" of SGCC (Grant No. XT71-12-028), Top & Tail Transformation Program (Grant No. EP/I031707/1), Science and Technology Project of the State Grid Corporation of China (Grant No. EPRIPDKJ [2012] 3185).

References

[1] Mu YF, Wu JZ, Ekanayake J, Jenkins N, Jia HJ. Primary frequency response from electric vehicles in the Great Britain power system. IEEE Trans Smart Grid 2013; 4(2): 1142–50.

[2] Ma YC, Houghton T, Cruden A, Infield D. Modeling the benefits of vehicle-to-grid technology to a power system. IEEE Trans Power Syst 2012; 27(2): 1012–20.

[3] EU Merge Project. Deliverable 2.1: Modelling Electric Storage devices for electric vehicles, 2010, Task. Rep.; 2010. http://www.ev-merge.eu/images/stories/uploads/MERGE_WP2_D2.1.pdf

[4] Qian KJ, Zhou CK, Allan M, Yuan Y. Modeling of load demand due to EV battery charging in distribution systems. IEEE Trans Power Syst 2011; 26(2): 802–10.

[5] Mu YF, Wu JZ, Jenkins N, Jia HJ, Wang CS. A spatial-temporal model for grid impact analysis of plug-in electric vehicles. Appl Energy 2014; 114(SI): 456–65.

[6] Tremblay O, Dessaint LA, Dekkiche AI. A generic battery model for the dynamic simulation of hybrid electric vehicles. IEEE Conference on Vehicle Power and Propulsion, Arlington, U.S.A, 2007.